

Improving Anomaly Segmentation with Multi-Granularity Cross-Domain Alignment

Ji Zhang

Southwest Jiaotong University,
Chengdu, China
Engineering Research Center of
Sustainable Urban Intelligent
Transportation, Ministry of Education
China
jizhang901@gmail.com

Xiao Wu*

Southwest Jiaotong University,
Chengdu, China
Engineering Research Center of
Sustainable Urban Intelligent
Transportation, Ministry of Education
China
wuxiaohk@gmail.com

Zhi-Qi Cheng

Language Technologies Institute,
School of Computer Science, Carnegie
Mellon University
Pittsburgh, United States
zhiqic@cs.cmu.edu

Qi He

Southwest Jiaotong University,
Chengdu, China
Engineering Research Center of
Sustainable Urban Intelligent
Transportation, Ministry of Education
China
qihe96@gmail.com

Wei Li

Southwest Jiaotong University,
Chengdu, China
Engineering Research Center of
Sustainable Urban Intelligent
Transportation, Ministry of Education
China
liwei@swjtu.edu.cn

ABSTRACT

Anomaly segmentation plays a crucial role in identifying anomalous objects within images, which facilitates the detection of road anomalies for autonomous driving. Although existing methods have shown impressive results in anomaly segmentation using synthetic training data, the domain discrepancies between synthetic training data and real test data are often neglected. To address this issue, the Multi-Granularity Cross-Domain Alignment (MGFDA) framework is proposed for anomaly segmentation in complex driving environments. It uniquely combines a new Multi-source Domain Adversarial Training (MDAT) module and a novel Cross-domain Anomaly-aware Contrastive Learning (CACL) method to boost the generality of the model, seamlessly integrating multi-domain data at both scene and sample levels. Multi-source domain adversarial loss and a dynamic label smoothing strategy are integrated into the MDAT module to facilitate the acquisition of domain-invariant features at the scene level, through adversarial training across multiple stages. CACL aligns sample-level representations with the contrastive loss on cross-domain data, which utilizes an anomaly-aware sampling strategy to efficiently sample hard samples and anchors. The proposed framework has decent properties of being parameter-free during the inference stage and is compatible with other anomaly segmentation networks. Experimental conducted

on Fishyscapes and RoadAnomaly datasets demonstrate that the proposed framework achieves state-of-the-art performance.

CCS CONCEPTS

• Computing methodologies → Image segmentation.

KEYWORDS

Anomaly segmentation; Domain adversarial training

ACM Reference Format:

Ji Zhang, Xiao Wu, Zhi-Qi Cheng, Qi He, and Wei Li. 2023. Improving Anomaly Segmentation with Multi-Granularity Cross-Domain Alignment. In *Proceedings of the 31st ACM International Conference on Multimedia (MM '23)*, October 29–November 3, 2023, Ottawa, ON, Canada. ACM, New York, NY, USA, 10 pages. <https://doi.org/10.1145/3581783.3611849>

1 INTRODUCTION

The development of deep learning has significantly advanced semantic segmentation [7, 10, 40, 47, 48] for autonomous driving [16, 17, 30, 35]. Unfortunately, since anomalous objects are usually diverse and versatile, which are commonly not included in the training data, the presence of anomalous objects in open-world scenarios (e.g. animals or rocks) poses great challenges for safety of autonomous driving. To address this issue, anomaly segmentation has been proposed [38], serving as a complementary approach to semantic segmentation. By incorporating anomaly segmentation, autonomous vehicles can effectively detect and identify anomalies presented on the road, enhancing the safety and reliability.

Anomaly data are relatively scarce and difficult to be collected, lacking sufficient data to train good deep models. To address this issue, previous anomaly segmentation methods [4, 21, 26, 34, 38, 52] synthesize training data by utilizing existing semantic segmentation datasets [12]. The training data are synthesized by labeling

*Corresponding author: Xiao Wu

Permission to make digital or hard copies of all or part of this work for personal or classroom use is granted without fee provided that copies are not made or distributed for profit or commercial advantage and that copies bear this notice and the full citation on the first page. Copyrights for components of this work owned by others than the author(s) must be honored. Abstracting with credit is permitted. To copy otherwise, or republish, to post on servers or to redistribute to lists, requires prior specific permission and/or a fee. Request permissions from [permissions@acm.org](https://www.acm.org/permissions).

MM '23, October 29–November 3, 2023, Ottawa, ON, Canada

© 2023 Copyright held by the owner/author(s). Publication rights licensed to ACM.
ACM ISBN 979-8-4007-0108-5/23/10...\$15.00
<https://doi.org/10.1145/3581783.3611849>

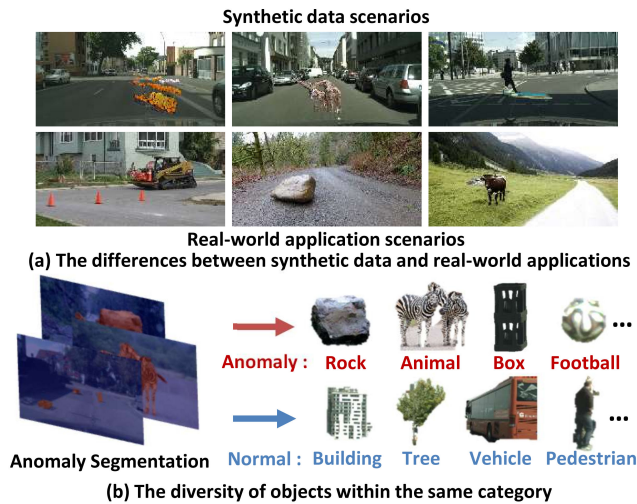


Figure 1: The challenges stem from the domain gap between the synthetic data and real-world applications and the diversity of objects within the same category.

infrequent objects as anomalies or cutting anomalous objects from outlier datasets and pasting them into original images [4, 52].

However, there exist huge domain differences and conspicuous data variabilities between the synthetic training data and the real-world applications. As shown in Fig. 1(a), the training data mostly consist of urban street scenes, while the anomaly segmentation datasets (e.g., FS LostAndFound [5] and RoadAnomaly [38] datasets) or real-world applications include a wider range of scenes, such as suburbs, plains and wilderness. The effectiveness of these methods is unsatisfactory when applied to real-world data. The models trained on synthetic training data may not generalize well to the scenes in anomaly segmentation datasets or real-world applications, especially in autonomous driving tasks where models may run in any scene.

Another crucial issue is that anomalous objects are usually diverse and versatile, posing challenges for anomaly segmentation models to learn compact sample distributions. Unlike semantic segmentation tasks where objects of the same category have similar characteristics, positive and negative samples in anomaly segmentation often have large intra-class differences. The positive samples refer to anomaly objects, such as rocks, animals, boxes and footballs, which have not been trained by semantic segmentation models. On the contrary, the negative samples are the categories used to train the models, including buildings, trees, vehicles, pedestrians and so on. The diversity of objects leads to distribution discrepancies between sample representations from synthetic data and those from real-world applications. Therefore, to adapt to real-world applications, it is necessary to address the scene discrepancy and sample distribution differences between the synthetic data and real-world applications.

In this paper, a Multi-Granularity Cross-Domain Alignment (MGCDA) framework is novelly proposed to enhance the generalization ability of anomaly segmentation, which is illustrated in Fig. 2. Multi-source Domain Adversarial Training (MDAT) module and Cross-domain Anomaly-aware Contrastive Learning (CACL)

method are integrated to align the differences between the synthetic data and real-world applications from both scene-level and sample distribution perspectives, respectively. A dissimilarity network [4] is first adopted to identify anomalous regions by detecting the differences between the original images and their reconstructed counterparts. MDAT is then proposed to facilitate the learning of domain-invariant features. A novel domain adversarial loss is employed to diminish the feature distribution distance of different training sets. The loss is executed in two stages within the network to alleviate the problem of gradient vanishing. A dynamic label smoothing technique is adopted to avoid the adversarial instability caused by the convergence of multi-domain training data distributions. To align the sample distribution differences, Cross-domain Anomaly-aware Contrastive Learning (CACL) is proposed to compute the pixel-wise contrastive loss, which involves picking anchors and samples from cross-domain data.

In addition, an anomaly-aware sampling strategy is integrated to select hard samples and anchors based on the predictions from the discriminator network. After integrating MDAT module and CACL into the proposed framework, a more powerful model is trained, leading to higher precision in anomaly segmentation. One charming property of the proposed framework is that it can enhance the model’s adaptability to unseen scenes without increasing the inference parameters. Moreover, the proposed framework is a general solution, which can be applied to the majority of anomaly segmentation approaches, acting as a plug-in.

The contributions are summarised as follows:

- Multi-Granularity Cross-Domain Alignment (MGCDA) framework is newly proposed to improve the generalizability of anomaly segmentation methods to real-world applications. It is a parameter-free solution during the inference stage, without increasing extra inference parameters. It is also compatible with other anomaly segmentation networks, acting as a plug-in to boost the performance.
- Multi-source domain adversarial training is proposed to mitigate scene-level differences. It incorporates a multi-source domain adversarial loss to facilitate the learning of domain-invariant features. Dynamic label smoothing strategy is employed to dynamically adjust domain labels as the feature distributions gradually fit each other.
- A new cross-domain anomaly-aware contrastive learning method is proposed to alleviate the differences in sample representations, which employs an anomaly-aware sampling strategy to sample hard anchors and samples based on the anomaly prediction results, so that contrastive loss can be efficiently computed across multiple training data.
- Extensive experiments conducted on the Fishyscapes benchmark [5] and the RoadAnomaly [38] dataset demonstrate that the proposed framework outperforms the state-of-the-art methods.

2 RELATED WORKS

2.1 Anomaly Segmentation

Existing methods [4, 21, 26, 34, 38, 52] for anomaly segmentation can be categorized into three categories: uncertainty-based, reconstruction-based and outlier exposure-based.

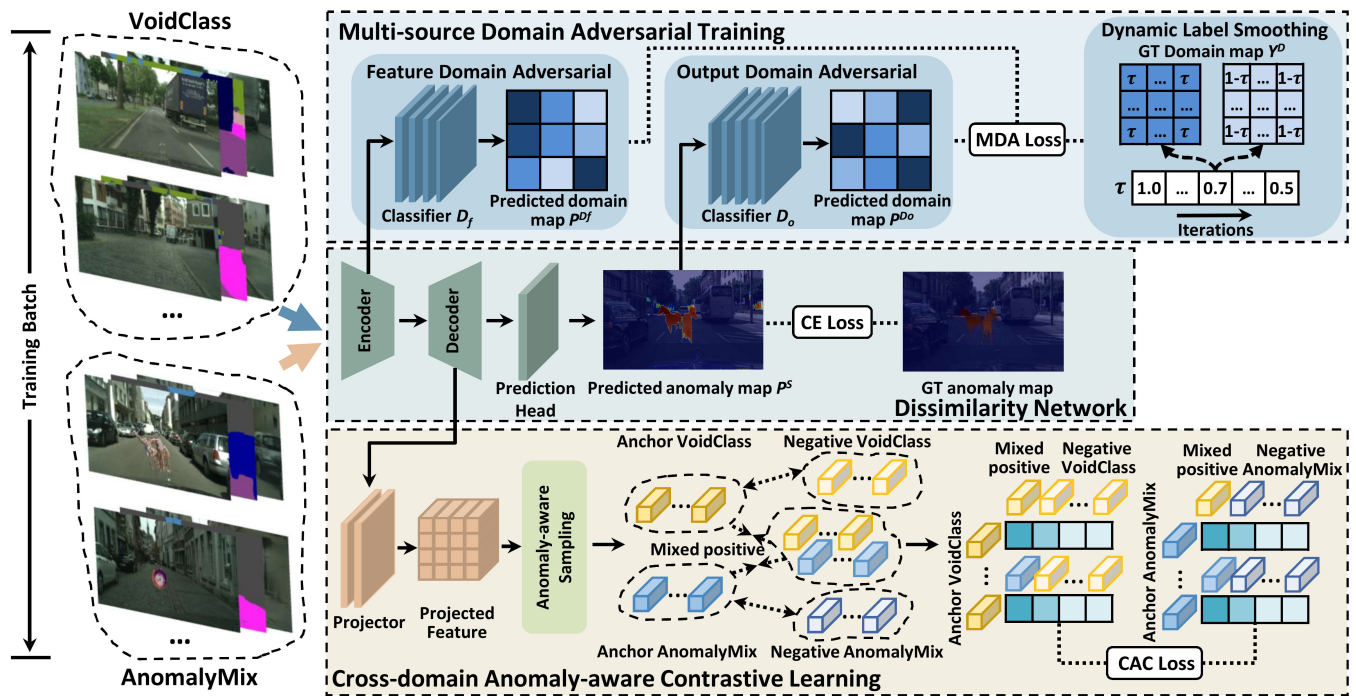


Figure 2: MGCDA framework consists of two key components: Multi-source Domain Adversarial Training (MDAT) module and Cross-domain Anomaly-aware Contrastive Learning (CACL) method. MDAT module performs domain adversarial training on multi-source data in two stages of the discriminative network. In addition, a dynamic label smoothing strategy is employed to dynamically adjust the domain label values. CACL method calculates the contrastive loss on pixels from cross-domain images, employing an anomaly-aware sampling technique to efficiently select anchor, positive and negative samples.

Uncertainty-based methods [26, 34] identify anomalous regions by predicting regions of high uncertainty. Earlier uncertainty-based methods [20, 33, 53] estimate uncertainty using predicted softmax values, which result in good performance in image-level tasks. However, these methods often inaccurately estimate the pixels at the boundaries of anomalous objects. To address this issue, the boundary suppression method was introduced by [25] and visual feature differences [44] are used to locate anomalous objects. Other methods [26, 29, 42] estimate uncertainty pixel by pixel to eliminate the impact of boundary pixels, but they have achieved lower accuracy in anomaly segmentation tasks.

An outlier exposure strategy (OE) [21] has been proposed to improve anomaly detection performance by using an auxiliary dataset of outliers. However, OE-based methods [2, 55] often require model retraining on an auxiliary dataset, which can affect the performance of the original segmentation network. To mitigate this issue, an auxiliary dataset is mixed with the original training set in [52].

Reconstruction-based methods [4, 38] reconstruct input images and compare them with the original images to find anomalous objects. Earlier methods [1] use autoencoders to regenerate original images, but the low-quality generated images limited their performance [38]. Recent methods [15, 38] reconstruct input images from semantic maps generated by segmentation networks. The performance of these methods is limited by the modeling ability of the dissimilarity network in capturing the differences between the original and generated images [4]. By introducing uncertainty maps in the

dissimilarity network, uncertainty-based and reconstruction-based methods are integrated into a single framework by [4]. Although previous anomaly segmentation methods achieve impressive results, the domain difference between synthetic training data and real test data has not been received enough attention. This motivates this paper to adopt multi-domain synthetic training data to improve the generalization ability of models in complex scenarios.

2.2 Domain Adversarial Training

Inspired by generative adversarial networks, adversarial training [6, 13, 22, 54, 58] has been widely studied in the fields of image classification, object detection, semantic segmentation, etc. It aims to enhance the generalization ability of the model by learning domain-invariant features across different domains. FCAN [22] was the first to apply adversarial training in semantic segmentation tasks, in which feature-level information is aligned. Features from the output space are aligned in [54], an approach that has been shown to be more effective than aligning intermediate features. Pixel-level adversarial learning is used by [6] to decouple image features and train the segmentation network with pure content information. However, these methods transfer models from labeled source domains to unlabeled target domains by utilizing unlabeled target domain data. In this work, the aim is to improve the generalization ability of models in real-world test data by using multiple labeled synthetic training data. Furthermore, the similarity of scenes among

multiple synthetic training data introduces additional challenges for adversarial training.

2.3 Contrastive learning

Contrastive learning is a feature learning paradigm that aims to minimize the distance between samples from the same class and maximize the distance between samples from different classes. Recently, unsupervised contrastive learning methods [8, 18, 57] have made significant progress, surpassing the previous pretext task based methods [31, 43]. A simple framework [8] is introduced to perform contrastive learning, where augmented views of the original image are used as positive samples and other images are used as negative samples. The memory bank strategy is adopted by [18] to store more negative samples. Supervised contrastive loss is designed by [24, 27] for image classification tasks. Furthermore, some methods [9, 11, 23, 46, 56, 60] have extended supervised contrastive loss to pixel-level semantic segmentation tasks. In [60], the segmentation network is pre-trained via intra-image contrastive loss and cross-image contrastive loss. [23, 56] utilize the memory bank to maintain a set of pixel embeddings or region embeddings averaged over classes. Multi-scale and cross-scale contrastive learning is adopted in [46]. In order to promote domain adaptation of semantic segmentation models on cross-domain data, [32] generates dynamic pseudo labels for target domain data to align the pixel-level features and prototypes of the same object class in target and source images. Unlike semantic segmentation tasks, both positive and negative samples in anomaly segmentation tasks exhibit large intra-class differences, which are further magnified in cross-domain data, posing significant challenges for existing pixel-level contrastive learning methods.

3 MULTI-GRANULARITY CROSS-DOMAIN ALIGNMENT

3.1 Framework

To alleviate the challenge of domain differences between synthetic data and real-world applications, a Multi-Granularity Cross-Domain Alignment (MGCDA) framework is proposed, the structure of which is shown in Fig. 2. The dissimilarity network as proposed in [4] is utilized to predict anomalous regions using input data, which includes original images, semantic maps and reconstructed images. The cross-entropy loss is then computed based on the predicted and ground-truth anomaly maps to guide the optimization of the network. A Multi-source Domain Adversarial Training (MDAT) method is proposed to eliminate domain differences at the scene level, in which a multi-source domain adversarial loss is designed to align the distributions more closely and a dynamic label smoothing strategy is employed to enhance training stability. To overcome gradient decay resulting from deeper network architectures, the MDAT method is applied separately in both the encoder and decoder stages of the network. Moreover, the Cross-domain Anomaly-aware Contrastive Learning (CACL) method is employed to align cross-domain sample representations by constructing a compact intra-class and discrete inter-class distribution. To lessen the computational burden, an Anomaly-aware Sampling strategy is incorporated into the CACL to efficiently sample hard examples and anchors based on anomaly segmentation results.

Specifically, the dissimilarity network consists of three components: an encoder, a decoder and a prediction head. A pre-trained VGG network [51] is used to encode the original and reconstructed images, while a simple CNN is employed to encode the semantic map. At each level of the feature pyramid, the input, synthesis and semantic feature maps are fused through a 1×1 convolution. The resulting feature map is correlated with the uncertainty map to focus on the areas with high uncertainty. The decoder decodes each feature map layer by layer and connects it with the corresponding higher-level feature map to generate the anomaly segmentation prediction. Spatial-aware normalization [45] is applied to ensure that the semantic information is not lost.

3.2 Training Data Synthesis

In this paper, the data generators proposed in [4, 52] are adopted to synthesize the training data for VoidClass and AnomalyMix, respectively. The training data in VoidClass is generated by labeling objects within the void class in the ground-truth semantic maps (e.g., Cityscapes [12]) as anomalous objects. Although the anomalous objects and scenes in VoidClass have a similar style, the scale and variety of anomalous objects are limited by the objects included in the void class. The training data in AnomalyMix are synthesized by selecting objects from the COCO dataset [37] as anomalous objects and pasting them onto images sampled from the Cityscapes training set. In AnomalyMix, anomalous objects with varying scales and types are introduced, but the style difference between anomalous objects and scenes often exists. Therefore, these two training data sets have domain differences and can complement each other. Following [4], the ground-truth anomaly maps are generated by labeling the anomalous objects area as 1, the void class (excluding the area selected as an anomalous object) as 255 and other areas as 0. The training data from VoidClass and AnomalyMix are defined as I_V and I_A , respectively.

3.3 Multi-source Domain Adversarial Training

Most existing domain adversarial training methods [6, 22, 54, 58], in dense prediction tasks, leverage unlabeled target domain data to facilitate domain adaptation from the source domain to the target domain, in which the adversarial loss is only calculated on target domain data. However, in anomaly segmentation tasks, the training sets can be synthesized using various methods, but the real-world test set is often unseen. In order to address this issue, a novel Multi-source Domain Adversarial Training (MDAT) method is proposed to utilize multiple source domain data for superior generalization to unseen target domains. The multi-source domain adversarial loss in MDAT aligns features from different source domains, aiming to make the distributions more similar, rather than just matching the target to the source domain features.

Due to the convergence of feature distributions from different source domains during the training process, traditional hard domain label assignment methods may not be conducive to stable model training [59]. A dynamic label smoothing strategy is designed to improve training stability by dynamically assigning values to domain labels. Additionally, to handle the inherent issues in anomaly segmentation, like gradient decay due to deeper network architectures, a multi-stage domain adversarial strategy has been implemented.

This strategy is applied separately in both the encoder and decoder stages of the network.

In MDAT, the features F generated by the encoder and the anomaly map P^S predicted by the dissimilarity network are fed into the feature domain classifier D_f and the output domain classifier D_o , respectively, yielding the predicted domain maps P^{Df} and P^{Do} . Furthermore, the ground-truth domain maps Y^D are generated by assigning domain label values of τ to the VoidClass and $1 - \tau$ to the AnomalyMix. The value of τ is dynamically determined through the label smoothing strategy during training, given by

$$\tau = \tau_b - (\tau_b - 0.5) \frac{i}{\max_i} \quad (1)$$

where τ_b is an initial hyperparameter set at the start of training and i represents the current number of training iterations.

With the predicted domain map P^{Df} and the ground-truth domain map Y^D , the multi-source domain adversarial loss of the feature domain classifier is computed as follows:

$$\mathcal{L}_{MDA}^{Df} = \frac{1}{N} \sum_{i=1}^N (P_V^{Df} - Y_A^D)^2 + (P_A^{Df} - Y_V^D)^2 \quad (2)$$

where N denotes the number of examples. P_V^{Df} and P_A^{Df} are domain maps predicted from images in VoidClass and AnomalyMix, respectively. The multi-source domain adversarial loss of the output domain classifier \mathcal{L}_{MDA}^{Do} can be computed in the similar way.

Specifically, the feature domain classifier is the sequential layers of four convolutions, which can be defined as $\{C_{ic/2,3}^1 - C_{ic/4,3}^1 - C_{ic/8,3}^1 - C_{1,3}\}$. $C_{oc,k}^s$ denotes the convolution layer with kernel of k and stride of s . The number of output channels is denoted by oc and ic is the number of input channels. The ReLU operation is applied after each convolution layer, except for the last one. Similarly, the output domain classifier is structured as $\{C_{32,3}^1 - C_{64,3}^1 - C_{128,3}^1 - C_{256,3}^1 - C_{1,3}\}$.

3.4 Cross-domain Anomaly-aware Contrastive Learning

In anomaly segmentation tasks, the vast diversity of anomalous objects creates substantial challenges in forming a coherent and well-structured sample distribution for modeling. Further complicating this, discrepancies in sample representations between synthetic data and real-world applications intensify the difficulty in aligning features of samples within the same category. Inspired by the promising outcomes achieved in various tasks by contrastive learning [8, 18], a novel Cross-domain Anomaly-aware Contrastive Learning (CACL) method is introduced. This approach aims to compact features from identical categories and separate features from different categories, thereby enabling models to establish a compact and discriminative distribution. In implementing CACL, each pixel within an image is considered a sample. pixels from anomalous regions are defined as positive samples, while those from non-anomalous regions are treated as negative samples. Nevertheless, the existence of marked differences between positive and negative samples across various domains may hinder the efficacy of contrastive loss, as it could become overwhelmed by numerous simple cases. To overcome this challenge, anchors are matched with positive samples from diverse domains and negative samples from

the same domain, facilitating contrastive learning on cross-domain data.

Given the granularity of the anomaly detection task, applying pixel-wise contrastive loss can be computationally demanding. In order to reduce computational complexity, several studies [23, 60] have leveraged sampling strategies or category prototype techniques. However, existing methods fall short in the anomaly segmentation task, owing to the extensive intra-class differences within samples of the same category. To overcome these shortcomings, an anomaly-aware sampling strategy is designed to effectively and efficiently select samples and anchors based on anomaly segmentation results, thus optimizing the execution of cross-domain pixel-wise contrastive loss. Inspired by the hard sample mining method [50], the proposed strategy identifies incorrectly predicted pixels as hard samples and correctly predicted ones as easy samples. To promote successful contrastive learning and prevent the model from falling into local minima, anchors are drawn from both hard and easy anomaly samples. Positive samples are then selectively chosen from easy anomaly samples to preclude pairing two hard anomaly samples (i.e., misclassified pixels), which could confuse the model. Likewise, negative samples are carefully picked from both hard and easy normal samples.

In CACL, the features generated by the decoder are transformed into a high-dimensional space using a projector, thus amplifying their ability to represent complex relationships. The anomaly-aware sampling strategy is employed to extract anchor, positive and negative sets from each image I_i ($i \in I^V \cup I^A$) within the training batch. These projected features are initially partitioned into the anomaly and normal regions in pixel space, utilizing the annotation details available in the ground-truth anomaly map. Leveraging the predicted anomaly map, both anomaly and normal regions are further dissected into hard and easy segments. From these hard and easy anomaly regions, N^a samples are chosen to constitute the anchor set S_i^a . Likewise, N^p samples are drawn exclusively from the easy anomaly region to assemble the positive set S_i^p , ensuring no overlap with S_i^a . N_h^n and N_e^n samples are obtained from the hard and easy normal regions, respectively, culminating in the negative set S_i^n . Ultimately, the same-domain anchor sets (S_V^a and S_A^a) and the same-domain negative sets (S_V^n and S_A^n) are expanded by consolidating the samples from images within the identical domain. Simultaneously, the cross-domain positive set ($S_{V \cup A}^p$) amalgamates the sampling outcomes from all domain images. Through this orchestrated process, the cross-domain anomaly-aware contrastive loss is formulated as follows:

$$\begin{aligned} \mathcal{L}_{CAC} = & - \frac{1}{|S_V^a|} \sum_{a \in S_V^a} \frac{1}{|S_{V \cup A}^p|} \sum_{p \in S_{V \cup A}^p} \frac{\exp^{a \cdot p / \alpha}}{\exp^{a \cdot p / \alpha} + \sum_{n \in S_V^n} \exp^{a \cdot n / \alpha}} \\ & - \frac{1}{|S_A^a|} \sum_{a \in S_A^a} \frac{1}{|S_{V \cup A}^p|} \sum_{p \in S_{V \cup A}^p} \frac{\exp^{a \cdot p / \alpha}}{\exp^{a \cdot p / \alpha} + \sum_{n \in S_A^n} \exp^{a \cdot n / \alpha}} \end{aligned} \quad (3)$$

where α is a temperature parameter. The projector is implemented as two 1×1 convolutions with Relu and can be defined as $\{C_{64,1}^1 - C_{128,1}^1\}$.

Table 1: Comparison with SOTA methods on Fishyscapes Leaderboard. The best and second are shown in bold and underlined, respectively.

Method	Venue	Re-training	OoD Data	FS LostAndFound		FS Static	
				AP(%)↑	FPR95(%)↓	AP(%)↑	FPR95(%)↓
MSP [19]	ICML'21	×	×	1.77	44.85	12.88	39.83
Entropy [20]	ICLR'17	×	×	2.93	44.83	15.41	39.75
Density-Minimum [5]	IJCV'21	×	×	4.25	47.15	62.14	17.43
Image Resynthesis++ [38]	ICCV'19	×	×	5.70	48.05	29.60	27.13
SML [25]	ICCV'21	×	×	31.05	21.52	53.11	19.64
Bayesian Deeplab [42]	Arxiv'18	✓	×	9.81	38.46	48.70	15.05
Logistic Regression [5]	IJCV'21	×	✓	4.65	24.36	57.16	13.39
Synboost [4]	CVPR'21	×	✓	43.22	15.79	72.59	18.75
PEBAL [52]	ECCV'22	×	✓	<u>44.17</u>	7.58	<u>92.38</u>	<u>1.73</u>
OoD training [5]	IJCV'21	✓	✓	10.29	22.11	45.00	19.40
Outlier Head [3]	GCPR'19	✓	✓	31.31	19.02	96.76	0.29
Dirichlet DeepLab [41]	NIPS'18	✓	✓	34.28	47.43	31.30	84.60
DenseHybrid [14]	ECCV'22	✓	✓	43.90	6.18	72.27	5.51
MGCDA	-	×	✓	60.96	<u>6.66</u>	74.97	17.71

Table 2: Comparison with SOTA methods on RoadAnomaly Dataset.

Method	Venue	AP(%)↑	FPR95(%)↓
Entropy [20]	ICLR'17	16.97	71.10
SML[25]	ICCV'21	17.52	70.70
MSP [19]	ICML'21	15.72	71.38
Max Logit [19]	ICML'21	18.98	70.48
Energy [39]	NIPS'20	19.54	70.17
GMMSeg-DeepLabV3+ [36]	NIPS'22	34.42	47.90
Synboost [4]	CVPR'21	38.21	64.75
PEBAL [52]	ECCV'22	<u>45.10</u>	<u>44.58</u>
MGCDA	-	50.35	42.19

3.5 Loss Function

The proposed framework is jointly optimized with the cross-entropy loss \mathcal{L}_{CE} , the multi-source domain adversarial losses \mathcal{L}_{MDA}^{Df} as well as \mathcal{L}_{MDA}^{Do} and the cross-domain anomaly-aware contrastive loss \mathcal{L}_{CAC} . The final loss function can be formulated as follows:

$$\mathcal{L}_{Total} = \mathcal{L}_{CE} + \lambda_f \mathcal{L}_{MDA}^{Df} + \lambda_o \mathcal{L}_{MDA}^{Do} + \lambda_c \mathcal{L}_{CAC} \quad (4)$$

where λ_f , λ_o and λ_c are parameters to balance the loss weights.

4 EXPERIMENTS

4.1 Datasets and Evaluation Metrics

To validate the efficacy of the method proposed in this paper, Experiments are conducted on the RoadAnomaly dataset and the Fishyscapes benchmark, both of which encompass two distinct scene datasets.

Fishyscapes [5] is a publicly accessible benchmark, specifically tailored for evaluating anomalies in semantic segmentation within urban driving scenarios. It is subdivided into two datasets: FS LostAndFound and FS Static. The FS LostAndFound dataset showcases real road anomalous objects and consists of a validation set with 100 images and a test set with 275 images. On the other hand, the FS Static dataset fuses anomalous objects from Pascal VOC into validation images from Cityscapes, comprising 60 images in the validation set and 1000 images in the test set.

RoadAnomaly [38] dataset features 60 real-world images, captured from various online sources, depicting unanticipated objects in proximity to vehicles, such as wildlife, debris, discarded tires, waste containers and construction machinery. These images were meticulously annotated at the pixel level to pinpoint the exact locations of the anomalous objects. Unlike the Fishyscapes benchmark, RoadAnomaly includes abnormal entities in a wide array of shapes and sizes, adding to its complexity. Every image in this dataset has been standardized to a resolution of 1280 × 720.

Evaluation Metrics. To foster a fair comparison with existing techniques, the same evaluation metrics utilized in the Fishyscapes benchmark [5] are employed for anomaly segmentation. The first metric, average precision (AP), gauges the model's aptitude in pixel-wise classification, reflecting its accuracy. The second metric, the false positive rate at a 95% true positive rate (FPR95), quantifies the model's suitability for safety-centric applications by analyzing the incidence of false positives at a recall rate of 95%.

4.2 Implementation Details

In order to fairly evaluate the effectiveness of the proposed framework, both the segmentation network and the generation network adopt the same network as [4], which is trained on Cityscapes dataset [12]. The dissimilarity network is trained for 50 epochs, using the Adam [28] optimizer with a learning rate of 0.0001. The polynomial schedule is adopted to adjust the learning rate, with a power of 0.99. The batch size is set to 8, with 4 training samples per domain. The training data are augmented by horizontal flipping and normalized using mean and standard deviation from Imagenet [49]. The domain label value τ_{base} is initialized to 1. λ_f , λ_o and λ_c are set to 0.04, 0.06 and 0.1, respectively. The optimal N^a is set to 50 through the hyper-parameter search. Empirically, N^p , N_h^n and N_e^n are set to $2N^a$, $2N^a$ and $6N^a$.

4.3 Comparisons with SOTA methods

The proposed method is compared with the state-of-the-art approaches on two real-world datasets, FS LostAndFound and RoadAnomaly, as well as a synthetic dataset, FS Static. For a fair comparison, following [5], these methods are classified, in Table 1, based

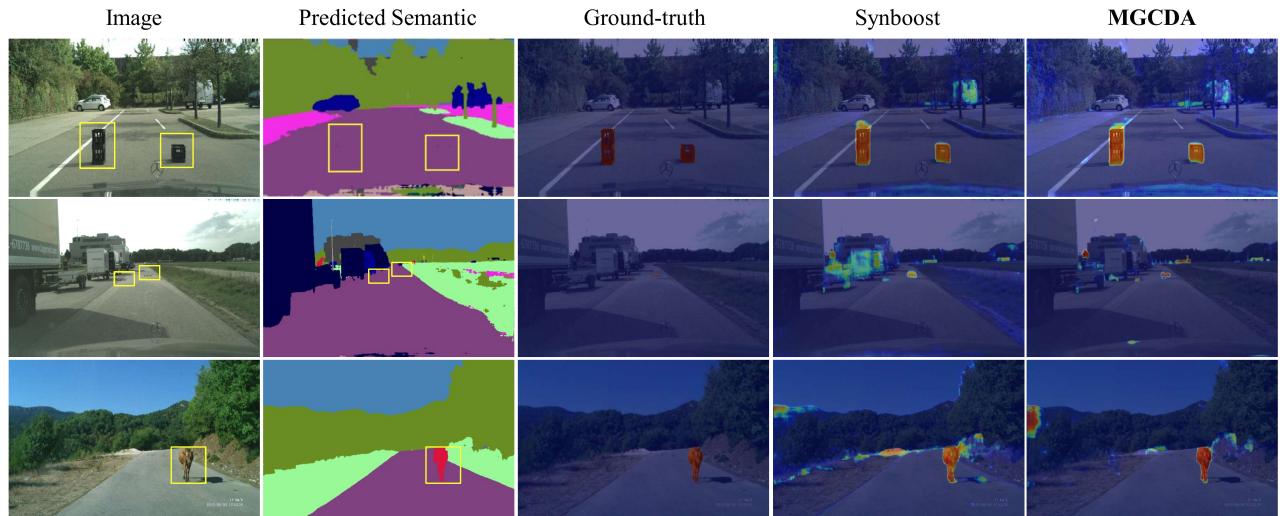


Figure 3: Visualization of the predicted anomaly maps on Fishyscapes benchmark and RoadAnomaly dataset. Anomaly objects in images are highlighted with a yellow box.

on whether they require re-training or utilize additional Out-of-Distribution (OoD) data.

As shown in Table 1, the proposed framework achieves a 16.79% improvement in AP performance with low FPR95 (6.66%) on FS LostAndFound dataset compared to previous methods. Previous methods [4, 52] trained models using synthetic training data. The domain differences between synthetic training data and FS LostAndFound make it difficult for previous methods to achieve high performance. Our framework significantly improves the generalization ability of the baseline [4] through the multi-source domain adversarial training module and the cross-domain anomaly-aware contrastive learning method, resulting in impressive results on FS LostAndFound. The experimental results of SOTA methods and the MGCDA framework on the RoadAnomaly dataset are listed in Table 2. The RoadAnomaly dataset is collected from the Internet, which has a wider range of scenarios and diverse objects than FS LostAndFound. Our framework improves the AP of the baseline method by 12.14% and reduces FPR95 by 22.56%, achieving the highest AP and the lowest FPR95. These results validate the general effectiveness of the proposed framework for real-world test sets in different domains.

Unlike FS LostAndFound, FS Static dataset is synthesized by pasting out-of-distribution objects on Cityscapes dataset [12], which has a high similarity with the synthetic training data. The highest performance on FS Static dataset is achieved by [3], which re-trains the entire semantic segmentation network on the synthetic training data. [52] fine-tunes the final classification block using the synthetic training data and also achieves good accuracy on FS Static dataset. Without retraining any network modules, the competitive results are obtained by the proposed framework, which demonstrates that extracting domain-invariant features and learning compact sample distributions also have a positive effect on the model’s performance on the same-domain data.

Overall, despite not reaching the peak in every metric, our model has achieved a remarkable performance boost, outperforming other

methods in three top results and one second-best result on real-world datasets. As shown in Fig. 3, Anomaly predictions by Synboost [4] and our method show an anomaly map with high scores (in yellow and red) for anomalous pixels, where our approach shows less false positive and false negative detections. Consequently, our method can detect unclear anomalies (row 3) more accurately than Synboost. Moreover, it still delivers commendable performance on synthetic data, emphasizing the benefits of improved generalization.

4.4 Ablation Studies

In this section, ablation studies are conducted on the Fishyscapes validation sets and RoadAnomaly dataset to demonstrate the effectiveness of the proposed module in Sec. 3. As mentioned above, the method proposed in [4] is adopted as the baseline.

4.4.1 Influence of extra training data. Three different training data are employed to train the baseline model to illustrate the influence of extra training data. *VoidClass* (or *AnomalyMix*) indicates that only the training data *VoidClass* (or *AnomalyMix*) is adopted in training. It should be noted that the baseline trained on *AnomalyMix* achieved high performance on FS Static, but failed on FS LostAndFound and RoadAnomaly datasets. This is mainly because the training data from *AnomalyMix* are synthesized by pasting anomaly objects, resulting in style difference between objects and scenes. The baseline overfits on finding areas with style differences, which affects the performance of anomaly segmentation. In addition, we directly mixed the data from both domains, denoted as *Mix*. Although more training data is added to training, the model’s performance decreased compared to training with only *VoidClass*. This result confirms the aforementioned viewpoint that data generated in different ways have domain differences and directly mixing these data will bias the model towards certain domain data, which fails to improve the generalization ability of the model.

4.4.2 Discussion of the multi-source domain adversarial training method. To validate the effectiveness of the proposed

Table 3: Ablation studies on Fishyscapes benchmark validation set and RoadAnomaly dataset.

Training Data	MDAT			CACL			FS LostAndFound		FS Static		RoadAnomaly	
	ODA	FDA	DLS	PCL	CPCL	AS	AP(%)↑	FPR95(%)↓	AP(%)↑	FPR95(%)↓	AP(%)↑	FPR95(%)↓
VoidClass							60.58	31.02	66.44	25.59	38.21	64.75
AnomalyMix							18.45	40.52	77.87	19.41	33.82	65.45
Mix							56.71	37.90	67.61	22.17	34.45	65.81
Multi-domain	✓						67.29	38.20	74.63	23.36	43.01	55.59
Multi-domain	✓	✓					68.99	25.39	76.56	21.95	45.24	56.33
Multi-domain	✓	✓	✓				70.20	25.76	78.05	26.12	46.17	53.89
Multi-domain	✓	✓	✓	✓			71.55	24.73	77.95	24.15	46.87	51.23
Multi-domain	✓	✓	✓		✓		72.30	22.15	78.79	17.15	47.95	48.29
Multi-domain	✓	✓	✓		✓	✓	74.71	19.08	80.90	22.72	50.35	42.19

multi-source domain adversarial training method, three network settings are compared. (a) *Baseline+ODA*: the output domain adversarial module is integrated into the baseline to utilize multi-domain training data for adversarial training. (b) *Baseline+ODA+FDA*: the feature domain adversarial module is introduced to form a multi-stage adversarial training framework. (c) *Baseline + MDAT*: the dynamic label smoothing strategy is employed to adjust the values of domain labels dynamically. As shown in Table 3, compared to the baseline trained with *Mix*, *Baseline + ODA* achieves 10.58% and 8.56% AP performance improvement on FS LostAndFound and RoadAnomaly datasets, respectively, with a slight decrease in performance on FS Static dataset. The obtained results affirm our hypothesis that domain differences exist between synthetic training data and real-world test data, and enhancing the model’s generalization capability can lead to improved performance on real-world applications. Furthermore, by adding the FDA module after the encoder, *Baseline + ODA + FDA* improves model performance, mainly due to the alleviation of the gradient decay. Finally, *Baseline + MMDAT* achieves performance improvements on all metrics across the three datasets. This indicates that the data from the two domains have certain similarities and the proposed dynamic label smoothing strategy can effectively stabilize the adversarial training process. Overall, the multi-source domain adversarial training method effectively enables the model to learn domain-invariant features from multi-domain data, thereby enhancing its generalization ability to different domain scenarios.

4.4.3 Effect of the Cross-domain Anomaly-aware Contrastive Learning method:

To verify the effect of CACL method, three network settings are compared. (d) *Baseline+MDAT+PCL*: Pixel-level contrastive loss [60] is introduced based on (c), in which a random sample strategy is integrated. (e) *Baseline + MDAT + CPCL*: Cross-domain pixel-level contrastive loss is employed to conduct contrastive learning on cross-domain data. (f) *Baseline+MDAT+CACL*: the anomaly-aware sampling strategy is employed to replace the random sample strategy and the complete multi-granularity cross-domain alignment framework is constructed. As shown in the last three rows of Table 3, the results show that our proposed method exhibits significant performance improvements, demonstrating the benefits of performing contrastive learning across domain data. Moreover, *Baseline + MDAT + CPCL* achieved significant improvements in AP on two real datasets and FPR95 is significantly reduced on all three datasets compared to *Baseline + MDAT*. This result

confirms the previous view that aligning sample distribution on cross-domain data can effectively improve the model’s robustness to samples from different domains. Due to the clear style differences between the pasted anomaly objects and the scene in FS Static dataset, there are a large number of redundant easy samples in the sample space, which results in little AP performance gain for CPCL method. By introducing the anomaly-aware sampling strategy, *Baseline+MMDAT+CACL* achieves the best results on all indicators (except FPR95 on FS Static), which indicates that the AS strategy can effectively alleviate the impact of redundant easy samples and can promote the more efficient execution of cross-domain pixel-level contrastive loss.

5 CONCLUSION

In this paper, a novel Multi-Granularity Cross-Domain Alignment (MGCDA) framework is proposed to address the challenge of domain differences between synthetic training data and real-world test data. The framework incorporates two new training modules, the Multi-source Domain Adversarial Training (MDAT) module and the Cross-domain Anomaly-aware Contrastive Learning (CACL) method, to improve the generalization capability of models. MDAT integrates a multi-source domain adversarial loss and a dynamic label smoothing strategy to leverage multi-source training data for domain adversarial training across multiple stages. CACL adopts an anomaly-aware sampling strategy to effectively and efficiently perform pixel-level contrastive loss on cross-domain data, so that the representations of cross-domain samples are aligned to improve the robustness of models. The proposed framework achieves significant improvements on two real datasets without adding any inference parameters and can be easily transferred to other anomaly segmentation networks.

ACKNOWLEDGMENTS

This work was supported in part by the National Natural Science Foundation of China (Grant No. 62001400), Key R&D Program of Guangxi Zhuang Autonomous Region, China (Grant No. AB22080038, AB22080039), Grant of the Institute of Applied Physics and Computational Mathematics, Beijing (Grant No. HXO2020-118), China Postdoctoral Science Foundation (Grant No. 2021M702713) and Fundamental Research Funds for the Central Universities (Grant No. 2682022JX007, 2682022KJ044, 2682022KJ056).

REFERENCES

- [1] Christoph Baur, Benedikt Wiestler, Shadi Albarqouni, and Nassir Navab. 2018. Deep Autoencoding Models for Unsupervised Anomaly Segmentation in Brain MR Images. In *Proceedings of the International MICCAI Brainlesion Workshop*, Vol. 11383. 161–169.
- [2] Petra Bevanic, Ivan Kreso, Marin Orsic, and Sinisa Segvic. 2018. Discriminative Out-of-Distribution Detection for Semantic Segmentation. *CoRR* abs/1808.07703 (2018).
- [3] Petra Bevanic, Ivan Kreso, Marin Orsic, and Sinisa Segvic. 2019. Simultaneous Semantic Segmentation and Outlier Detection in Presence of Domain Shift. In *Proceedings of the German Conference on Pattern Recognition*, Vol. 11824. 33–47.
- [4] Giancarlo Di Biase, Hermann Blum, Roland Siegwart, and César Cadena. 2021. Pixel-Wise Anomaly Detection in Complex Driving Scenes. In *Proceedings of the IEEE Conference on Computer Vision and Pattern Recognition*. 16918–16927.
- [5] Hermann Blum, Paul-Edouard Sarlin, Juan I. Nieto, Roland Siegwart, and Cesar Cadena. 2021. The Fishyscapes Benchmark: Measuring Blind Spots in Semantic Segmentation. *Int. J. Comput. Vis.* 129, 11 (2021), 3119–3135.
- [6] Wei-Lun Chang, Hui-Po Wang, Wen-Hsiao Peng, and Wei-Chen Chiu. 2019. All About Structure: Adapting Structural Information Across Domains for Boosting Semantic Segmentation. In *Proceedings of the IEEE Conference on Computer Vision and Pattern Recognition*. 1900–1909.
- [7] Liang-Chieh Chen, George Papandreou, Iasonas Kokkinos, Kevin Murphy, and Alan L. Yuille. 2018. DeepLab: Semantic Image Segmentation with Deep Convolutional Nets, Atrous convolution, and Fully Connected CRFs. *IEEE Trans. Pattern Anal. Mach. Intell.* 40, 4 (2018), 834–848.
- [8] Ting Chen, Simon Kornblith, Mohammad Norouzi, and Geoffrey E. Hinton. 2020. A Simple Framework for Contrastive Learning of Visual Representations. In *Proceedings of the International Conference on Machine Learning*, Vol. 119. PMLR, 1597–1607.
- [9] Zhi-Qi Cheng, Qi Dai, Hong Li, Jingkuan Song, Xiao Wu, and Alexander G Hauptmann. 2022. Rethinking spatial invariance of convolutional networks for object counting. In *IEEE/CVF Conference on Computer Vision and Pattern Recognition*. 19638–19648.
- [10] Zhi-Qi Cheng, Qi Dai, Siyao Li, Teruko Mitamura, and Alexander Hauptmann. 2022. Gsrformer: Grounded Situation Recognition Transformer with Alternate Semantic Attention Refinement. In *Proceedings of the ACM International Conference on Multimedia*. 3272–3281.
- [11] Zhi-Qi Cheng, Jun-Xiu Li, Qi Dai, Xiao Wu, and Alexander G Hauptmann. 2019. Learning spatial awareness to improve crowd counting. In *IEEE/CVF international conference on computer vision*. 6152–6161.
- [12] Marius Cordts, Mohamed Omran, Sebastian Ramos, Timo Rehfeld, Markus Enzweiler, Rodrigo Benenson, Uwe Franke, Stefan Roth, and Bernt Schiele. 2016. The Cityscapes Dataset for Semantic Urban Scene Understanding. In *Proceedings of the IEEE Conference on Computer Vision and Pattern Recognition*. 3213–3223.
- [13] Yaroslav Ganin and Victor S. Lempitsky. 2015. Unsupervised Domain Adaptation by Backpropagation. In *Proceedings of the International Conference on Machine Learning*, Vol. 37. 1180–1189.
- [14] Matej Grcic, Petra Bevanic, and Sinisa Segvic. 2022. DenseHybrid: Hybrid Anomaly Detection for Dense Open-Set Recognition. In *Proceedings of the European Conference on Computer Vision*, Vol. 13685. Springer, 500–517.
- [15] David Haldimann, Hermann Blum, Roland Siegwart, and Cesar Cadena. 2019. This is not what I imagined: Error Detection for Semantic Segmentation through Visual Dissimilarity. *CoRR* abs/1909.00676 (2019).
- [16] Alexander Hauptmann, Lijun Yu, Wenhe Liu, Yijun Qian, Zhiqi Cheng, Liangke Gui, et al. 2023. Robust Automatic Detection of Traffic Activity. (2023).
- [17] Jun-Yan He, Zhi-Qi Cheng, Chenyang Li, Wangmeng Xiang, Binghui Chen, Bin Luo, Yifeng Geng, and Xuansong Xie. 2023. DAMO-StreamNet: Optimizing Streaming Perception in Autonomous Driving. *CoRR* abs/2303.17144 (2023).
- [18] Kaiming He, Haoqi Fan, Yuxin Wu, Saining Xie, and Ross B. Girshick. 2020. Momentum Contrast for Unsupervised Visual Representation Learning. In *Proceedings of the IEEE Conference on Computer Vision and Pattern Recognition*.
- [19] Dan Hendrycks, Steven Basart, Mantas Mazeika, Andy Zou, Joseph Kwon, Mohammadreza Mostajabi, Jacob Steinhardt, and Dawn Song. 2022. Scaling Out-of-Distribution Detection for Real-World Settings. In *Proceedings of the International Conference on Machine Learning*, Vol. 162. 8759–8773.
- [20] Dan Hendrycks and Kevin Gimpel. 2017. A Baseline for Detecting Misclassified and Out-of-Distribution Examples in Neural Networks. In *Proceedings of the International Conference on Learning Representations*.
- [21] Dan Hendrycks, Mantas Mazeika, and Thomas G. Dietterich. 2019. Deep Anomaly Detection with Outlier Exposure. In *Proceedings of the International Conference on Learning Representations*.
- [22] Judy Hoffman, Dequan Wang, Fisher Yu, and Trevor Darrell. 2016. FCNs in the Wild: Pixel-level Adversarial and Constraint-based Adaptation. *CoRR* abs/1612.02649 (2016).
- [23] Hanzhe Hu, Jinshi Cui, and Liwei Wang. 2021. Region-aware Contrastive Learning for Semantic Segmentation. In *Proceedings of the IEEE International Conference on Computer Vision*. 16271–16281.
- [24] Ting-Yao Hu, Zhi-Qi Cheng, and Alexander G Hauptmann. 2021. Subspace representation learning for few-shot image classification. *arXiv preprint arXiv:2105.00379* (2021).
- [25] Sanghun Jung, Jungsoo Lee, Daehoon Gwak, Sungha Choi, and Jaegul Choo. 2021. Standardized Max Logits: A Simple yet Effective Approach for Identifying Unexpected Road Obstacles in Urban-Scene Segmentation. In *Proceedings of the IEEE International Conference on Computer Vision*. 15405–15414.
- [26] Alex Kendall and Yarin Gal. 2017. What Uncertainties Do We Need in Bayesian Deep Learning for Computer Vision?. In *Proceedings of Advances in Neural Information Processing Systems*. 5574–5584.
- [27] Prannay Khosla, Piotr Teterwak, Chen Wang, Aaron Sarna, Yonglong Tian, Phillip Isola, Aaron Maschiot, Ce Liu, and Dilip Krishnan. 2020. Supervised Contrastive Learning. *CoRR* abs/2004.11362 (2020).
- [28] Diederik P. Kingma and Jimmy Ba. 2015. Adam: A Method for Stochastic Optimization. In *Proceedings of the International Conference on Learning Representations*.
- [29] Balaji Lakshminarayanan, Alexander Pritzel, and Charles Blundell. 2017. Simple and Scalable Predictive Uncertainty Estimation using Deep Ensembles. In *Proceedings of Advances in Neural Information Processing Systems*. 6402–6413.
- [30] Jin-Peng Lan, Zhi-Qi Cheng, Jun-Yan He, Chenyang Li, Bin Luo, Xu Bao, Wangmeng Xiang, Yifeng Geng, and Xuansong Xie. 2023. Procontext: Exploring progressive context transformer for tracking. In *IEEE International Conference on Acoustics, Speech and Signal Processing*. IEEE, 1–5.
- [31] Gustav Larsson, Michael Maire, and Gregory Shakhnarovich. 2016. Learning Representations for Automatic Colorization. In *Proceedings of the European Conference on Computer Vision*, Vol. 9908. 577–593.
- [32] Geon Lee, Chanho Eom, Wonkyung Lee, Hyekang Park, and Bumsuh Ham. 2022. Bi-directional Contrastive Learning for Domain Adaptive Semantic Segmentation. In *Proceedings of the European Conference on Computer Vision*, Vol. 13690. 38–55.
- [33] Kimin Lee, Honglak Lee, Kibok Lee, and Jinwoo Shin. 2018. Training Confidence-calibrated Classifiers for Detecting Out-of-Distribution Samples. In *Proceedings of the International Conference on Learning Representations*.
- [34] Kimin Lee, Kibok Lee, Honglak Lee, and Jinwoo Shin. 2018. A Simple Unified Framework for Detecting Out-of-Distribution Samples and Adversarial Attacks. In *Proceedings of Advances in Neural Information Processing Systems*. 7167–7177.
- [35] Chenyang Li, Zhi-Qi Cheng, Jun-Yan He, Pengyu Li, Bin Luo, Hanyuan Chen, Yifeng Geng, Jin-Peng Lan, and Xuansong Xie. 2023. Longshortnet: Exploring temporal and semantic features fusion in streaming perception. In *IEEE International Conference on Acoustics, Speech and Signal Processing*. IEEE, 1–5.
- [36] Chen Liang, Wenguan Wang, Jiaxu Miao, and Yi Yang. 2022. GMMSeg: Gaussian Mixture based Generative Semantic Segmentation Models. In *Proceedings of Advances in Neural Information Processing Systems*.
- [37] Tsung-Yi Lin, Michael Maire, Serge J. Belongie, James Hays, Pietro Perona, Deva Ramanan, Piotr Dollár, and C. Lawrence Zitnick. 2014. Microsoft COCO: Common Objects in Context. In *Proceedings of the European Conference on Computer Vision*, Vol. 8693. 740–755.
- [38] Krzysztof Lis, Krishna Kanth Nakka, Pascal Fua, and Mathieu Salzmann. 2019. Detecting the Unexpected via Image Resynthesis. In *Proceedings of the IEEE International Conference on Computer Vision*. 2152–2161.
- [39] Weitang Liu, Xiaoyun Wang, John D. Owens, and Yixuan Li. 2020. Energy-based Out-of-distribution Detection. In *Proceedings of Advances in Neural Information Processing Systems*.
- [40] Jonathan Long, Evan Shelhamer, and Trevor Darrell. 2015. Fully Convolutional Networks for Semantic Segmentation. In *Proceedings of the IEEE Conference on Computer Vision and Pattern Recognition*. 3431–3440.
- [41] Andrey Malinin and Mark J. F. Gales. 2018. Predictive Uncertainty Estimation via Prior Networks. In *Proceedings of Advances in Neural Information Processing Systems*. 7047–7058.
- [42] Jishnu Mukhoti and Yarin Gal. 2018. Evaluating Bayesian Deep Learning Methods for Semantic Segmentation. *CoRR* abs/1811.12709 (2018).
- [43] Mehdi Norouzi and Paolo Favaro. 2016. Unsupervised Learning of Visual Representations by Solving Jigsaw Puzzles. In *Proceedings of the European Conference on Computer Vision*, Vol. 9910. 69–84.
- [44] Philipp Oberdiek, Matthias Rottmann, and Gernot A. Fink. [n. d.]. Detection and Retrieval of Out-of-Distribution Objects in Semantic Segmentation. In *Proceedings of the IEEE Conference on Computer Vision and Pattern Recognition (Workshops)*.
- [45] Taesung Park, Ming-Yu Liu, Ting-Chun Wang, and Jun-Yan Zhu. 2019. Semantic Image Synthesis With Spatially-Adaptive Normalization. In *Proceedings of the IEEE Conference on Computer Vision and Pattern Recognition*. 2337–2346.
- [46] Theodoros Pissas, Claudio S. Rivasio, Lyndon Da Cruz, and Christos Bergeles. 2022. Multi-scale and Cross-scale Contrastive Learning for Semantic Segmentation. In *Proceedings of the European Conference on Computer Vision*, Vol. 13689. 413–429.
- [47] Jian-Jun Qiao, Zhi-Qi Cheng, Xiao Wu, Wei Li, and Ji Zhang. 2022. Real-time Semantic Segmentation with Parallel Multiple Views Feature Augmentation. In *Proceedings of the ACM International Conference on Multimedia*. 6300–6308.
- [48] Jian-Jun Qiao, Xiao Wu, Jun-Yan He, Wei Li, and Qiang Peng. 2022. SWNet: A Deep Learning Based Approach for Splashed Water Detection on Road. *IEEE Transactions on Intelligent Transportation Systems* 23, 4 (2022), 3012–3025.

- [49] Olga Russakovsky, Jia Deng, Hao Su, Jonathan Krause, Sanjeev Satheesh, Sean Ma, Zhiheng Huang, Andrej Karpathy, Aditya Khosla, Michael S. Bernstein, Alexander C. Berg, and Li Fei-Fei. 2015. ImageNet Large Scale Visual Recognition Challenge. *Int. J. Comput. Vis.* 115, 3 (2015), 211–252.
- [50] Abhinav Shrivastava, Abhinav Gupta, and Ross B. Girshick. 2016. Training Region-Based Object Detectors with Online Hard Example Mining. In *Proceedings of the IEEE Conference on Computer Vision and Pattern Recognition*. 761–769.
- [51] Karen Simonyan and Andrew Zisserman. 2015. Very Deep Convolutional Networks for Large-Scale Image Recognition. In *Proceedings of the International Conference on Learning Representations*.
- [52] Yu Tian, Yuyuan Liu, Guansong Pang, Fengbei Liu, Yuanhong Chen, and Gustavo Carneiro. 2022. Pixel-Wise Energy-Biased Abstention Learning for Anomaly Segmentation on Complex Urban Driving Scenes. In *Proceedings of the European Conference on Computer Vision*, Vol. 13699. 246–263.
- [53] Yu Tian, Guansong Pang, Yuanhong Chen, Rajvinder Singh, Johan W. Verjans, and Gustavo Carneiro. 2021. Weakly-supervised Video Anomaly Detection with Robust Temporal Feature Magnitude Learning. In *Proceedings of the IEEE International Conference on Computer Vision*. 4955–4966.
- [54] Yi-Hsuan Tsai, Wei-Chih Hung, Samuel Schuster, Kihyuk Sohn, Ming-Hsuan Yang, and Manmohan Chandraker. 2018. Learning to Adapt Structured Output Space for Semantic Segmentation. In *Proceedings of the IEEE Conference on Computer Vision and Pattern Recognition*. 7472–7481.
- [55] Simon Vandenhende, Stamatios Georgoulis, Marc Proesmans, Dengxin Dai, and Luc Van Gool. 2020. Revisiting Multi-Task Learning in the Deep Learning Era. *CoRR* abs/2004.13379 (2020).
- [56] Wenguan Wang, Tianfei Zhou, Fisher Yu, Jifeng Dai, Ender Konukoglu, and Luc Van Gool. 2021. Exploring Cross-Image Pixel Contrast for Semantic Segmentation. In *Proceedings of the IEEE International Conference on Computer Vision*. 7283–7293.
- [57] Zhirong Wu, Yuanjun Xiong, Stella X. Yu, and Dahua Lin. 2018. Unsupervised Feature Learning via Non-Parametric Instance Discrimination. In *Proceedings of the IEEE Conference on Computer Vision and Pattern Recognition*. 3733–3742.
- [58] Fei Yu, Mo Zhang, Hexin Dong, Sheng Hu, Bin Dong, and Li Zhang. 2021. DAST: Unsupervised Domain Adaptation in Semantic Segmentation Based on Discriminator Attention and Self-Training. In *Proceedings of the AAAI Conference on Artificial Intelligence*. 10754–10762.
- [59] Yifan Zhang, Xue Wang, Jian Liang, Zhang Zhang, Liang Wang, Rong Jin, and Tieniu Tan. 2023. Free Lunch for Domain Adversarial Training: Environment Label Smoothing. *CoRR* abs/2302.00194 (2023).
- [60] Xiangyun Zhao, Raviteja Vemulapalli, Philip Andrew Mansfield, Boqing Gong, Bradley Green, Lior Shapira, and Ying Wu. 2021. Contrastive Learning for Label Efficient Semantic Segmentation. In *Proceedings of the IEEE International Conference on Computer Vision*. 10603–10613.